

AD-A134 929

~~78-0267~~

①

CCDs FOR SPEECH BANDWIDTH REDUCTION

C. R. Hewes

Texas Instruments Incorporated

April 1978

Semiannual Technical Report
Contract No. N00173-77-C-0100
18 April 1977 - 18 October 1978

DTIC
FILE
NOV 25 1983
H

Sponsored by
Defense Advanced Research Projects Agency
DARPA Order No. 3335

APPROVED FOR PUBLIC RELEASE
DISTRIBUTION UNLIMITED

The views and conclusions contained in this document are those of the author and should not be interpreted as necessarily representing the official policies, either expressed or implied, of the Defense Advanced Research Projects Agency or the U. S. Government.

DTIC FILE COPY

83 11 25 021

TABLE OF CONTENTS

<u>SECTION</u>		<u>PAGE</u>
I	INTRODUCTION.	1
II	ANALYZER IC	3
	A. CCD Bandpass Filter.	3
	B. CCD Topology	8
	C. CCD Filter Amplifier	15
	D. Full-Wave Rectifier.	18
	E. Low-Pass Filter.	25
	F. Logarithmic A/D Converter.	25
	G. MOS/TTL Output Buffers	29
III	SYNTHESIZER	31
IV	STATUS AND PLANS.	34

LIST OF TABLES

<u>TABLE</u>		<u>PAGE</u>
1	Belgard Filter Banks.	5
2	DCI Amplifier Characteristics	21

LIST OF ILLUSTRATIONS

<u>FIGURE</u>		<u>PAGE</u>
1	Block Diagram of a Belgard Channel Vocoder.	2
2	Analysis IC	4
3	Belgard Analyzer Filter Bank.	6
4	Analyzer Filter #6.	7
5	Analyzer Channel #6 Showing the Effects of Tapweight Roundoff.	9
6	Weighting Coefficients for Analyzer Filter #6	10
7	Analyzer Filter #17	11
8	Analyzer Filter #17 with Tapweight Roundoff	12
9	Tapweights of Filter #17.	13
10	Schematic of CCD Charge Transfer Process and Clock Timing	14

LIST OF ILLUSTRATIONS
(continued)

<u>FIGURE</u>		<u>PAGE</u>
11	CCD Output Circuit.	16
12	Amplifier/Rectifier	17
13	Amplifier Open Loop Frequency Response.	19
14	Amplifier Closed Loop Frequency Response.	20
15	Full-Wave Rectifier Circuit and Timing Diagram.	23
16	Rectifier Output Waveform from Breadboard Simulation.	24
17	Low-Pass Filter	26
18	Five-Bit Logarithmic A/D Converter.	28
19	MOS to TTL Output Buffers	30
20	Synthesis IC.	32
21	Two-Pole Bandpass Filter.	33
22	Belgard Chip Development Schedule	35

SECTION I
INTRODUCTION

This report concerns the progress to date in the development of analog CCD devices to be used in the implementation of a highly integrated, potentially low-cost version of the Belgard channel vocoder algorithm. This interim report will describe both the voice analyzer and synthesizer IC topologies, but will concentrate on the design details of only the analyzer IC which is nearing completion of the design phase.

A simplified block diagram of the Belgard vocoder is shown in Figure 1. In the first demonstration the two portions of the system enclosed by dashed lines will be custom CCD/MOS LSI circuits, one for speech analysis and one for speech synthesis, that are the subject of the current contract. The pre-sampling and preemphasis filters are relatively simple analog filters that ultimately can be included in the analyzer IC. The pitch extraction, framing, and encoding will be implemented digitally using microcomputer.

At the receiving end a microcomputer will decode the digital information and send twenty eight-bit digital words to the synthesizer IC per frame. One of the eight-bit words contains the voiced/unvoiced decisions and the pitch period. The excitation word is recognized by the presence of nonzero bits in the three MSB lines and controls the excitation generator which produces pitch pulses or random noise. The other 19 words contain the channel gains in log PCM form. These words are D/A converted, sampled and held, and interpolated by low pass filters to provide a gain control signal for each of the 19 channels. A summing amplifier provides a sampled-and-held audio output signal.

In Section II of this report we will describe the various circuit functions of the analyzer IC. In Section III the synthesizer IC is outlined. Section IV will detail our schedule and plans for the remainder of the program.

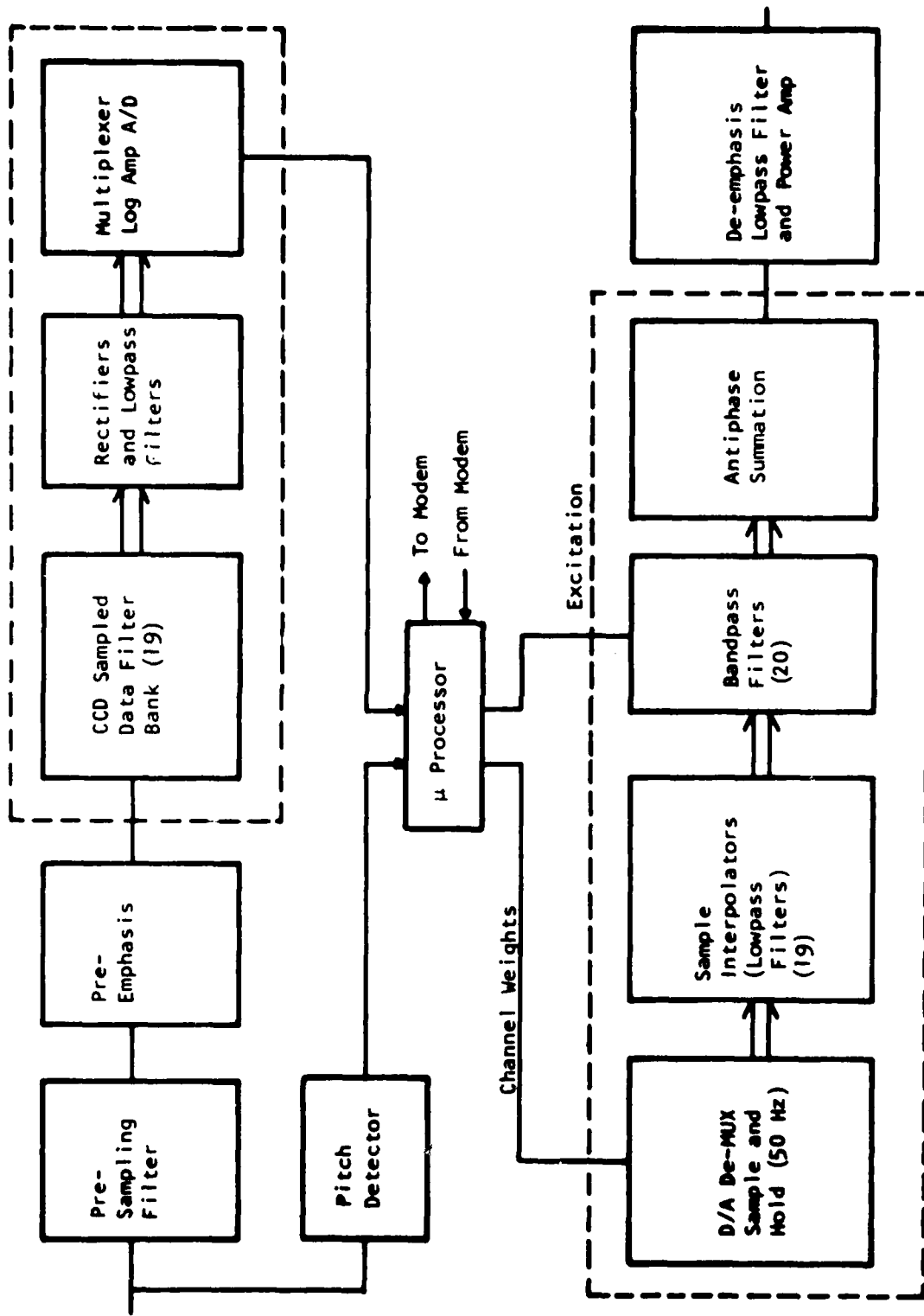


Figure 1 Block Diagram of a Belgard Channel Vocoder. The dashed lines enclose the analysis and synthesis ICs which are being developed.

SECTION II
ANALYZER IC

In this section we discuss some specific details of the various components of the Belgard analyzer IC that is shown in Figure 2. In 11.A we describe the filter characteristics to be used in the bandpass filter bank. In 11.B the CCD filters are discussed, and the other circuits are described in 11.C, 11.D, 11.E, 11.F, and 11.G.

A. CCD Bandpass Filters

Early analysis indicated that CCD transversal filters would provide a silicon area efficient approach to fabricating the Belgard filter band. Table 1 shows both the analyzer and synthesizer filter center frequencies and bandwidth, and the Belgard filter characteristics are plotted in Figure 3. The original Belgard system used recursive Butterworth filters (three complex pole pairs) that we cannot exactly match with CCD transversal filters. As described in more detail below, we will match the Butterworth characteristics from the center of each band down to about -20 dB. Outside this region the CCD filters will fall off much more rapidly than Butterworth characteristics, but our stopband attenuation will be limited to about -50 dB. Discussions with Lincoln Laboratory indicate that these characteristics will be acceptable. The sharper filtering may perhaps be desirable and Lincoln simulations of 50 dB stopband levels prove that no performance degradation can be detected with this stopband level.

The CCD FIR filter weighting coefficients are designed using the Parks, McClellan, Rabiner design program with appropriate subroutine modifications to model the Butterworth response characteristics.

Typical of the low frequency channels are the frequency characteristics of channel #6 that are plotted in Figure 4. Both the Butterworth (smooth curve) and the 100-stage CCD FIR characteristics are shown. The FIR response

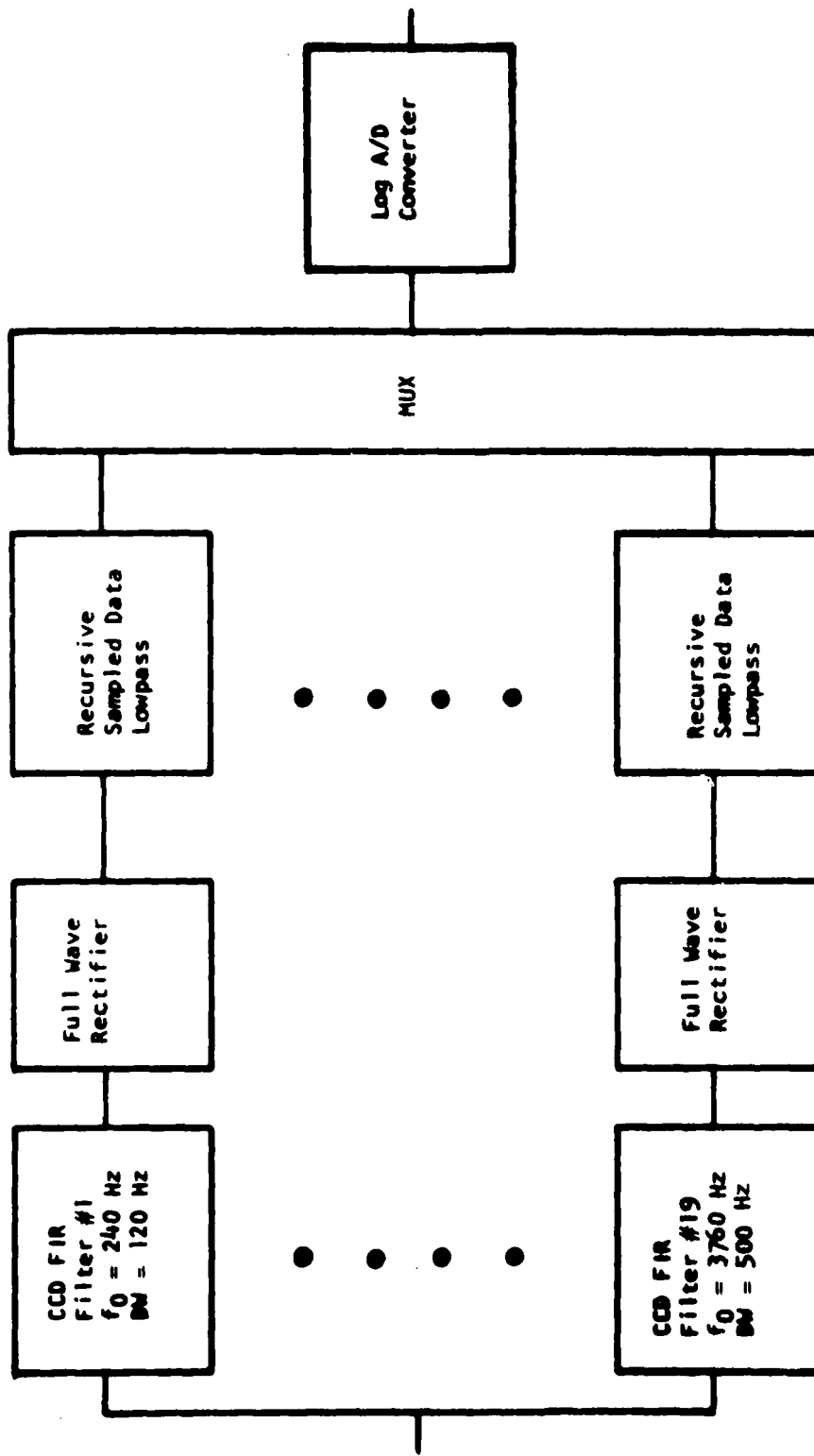


Figure 2 Analysis IC

TABLE 1
BELGARD FILTER BANKS

<u>Channel Number</u>	<u>Center Frequency (Hertz)</u>	<u>Analyzer Bandwidth (Hertz)</u>	<u>Synthesizer Bandwidth (Hertz)</u>
1	240	120	40
2	360	120	40
3	480	120	40
4	600	120	40
5	720	120	40
6	840	120	40
7	1000	150	40
8	1150	150	40
9	1300	150	40
10	1450	150	40
11	1600	150	40
12	1800	200	60
13	2000	200	60
14	2200	200	60
15	2400	200	60
16	2700	300	60
17	3000	300	60
18	3700	300	60
19	3760	500	¹ 60 f _o = 3600
19a	3750		² 500 f _o = 3750

¹ Voiced

² Unvoiced

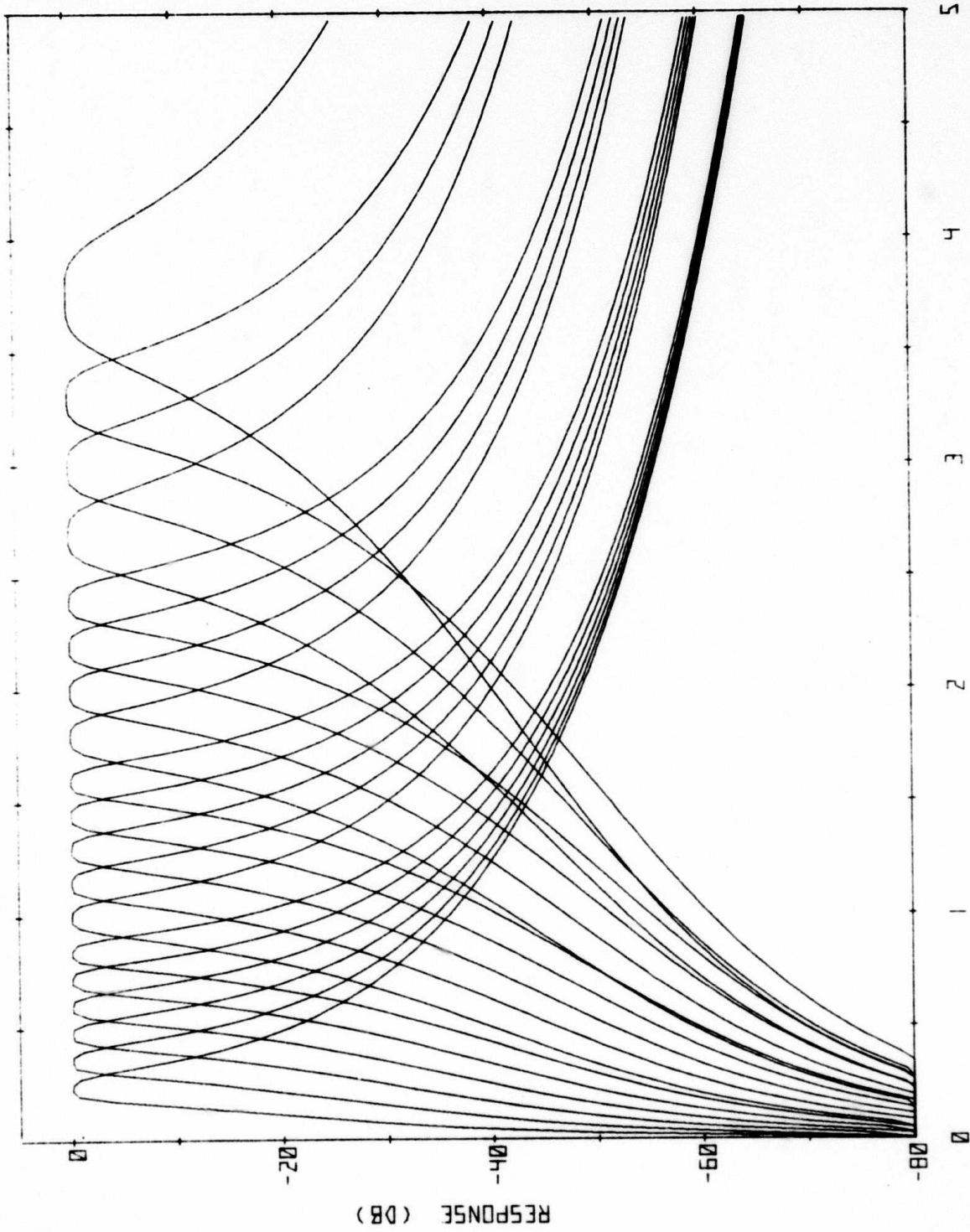
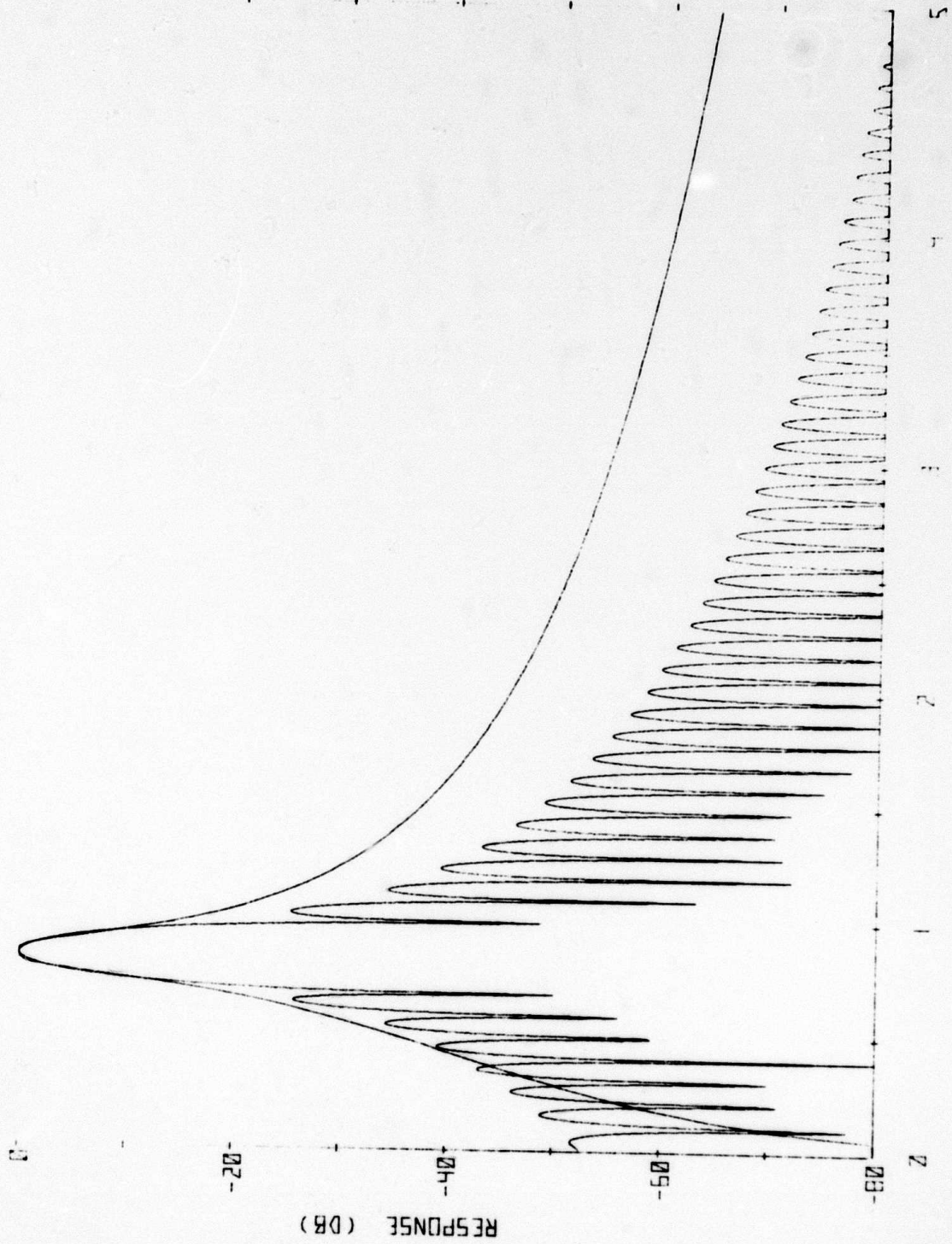


Figure 3 Belgard Analyzer Filter Bank



FREQUENCY (KHZ)

Figure 4 Analyzer Filter #6. The Butterworth characteristic (smooth curve) and the FIR characteristic are both shown.

matches the Butterworth within 0.4 dB in the band center, and in the stopband the ripple is weighted by the reciprocal of the Butterworth response in the design program to yield a sidelobe response somewhat below the Butterworth throughout most of the audio frequency band. The effects of weighting coefficient roundoff (which is required by the photomask fabrication equipment) can be seen by comparing Figures 4 and 5. The roundoff to the nearest of the 500 available increments results in nonuniform sidelobe structures with peaks in the -60 dB range for this filter as seen in Figure 5. The impulse response of filter #6 can be seen in Figure 6.

The frequency response of the high frequency channels (#17) is shown in Figures 7 and 8. As in channel #6 the roundoff limits sidelobe response, this time to about -50 dB. The bandwidth of this filter is wider than #6, resulting in less processing gain and greater sensitivity to roundoff error. The impulse response plot in Figure 9 reveals a larger proportion of very small weights, which is consistent with the greater roundoff sensitivity.

These two filters represent extremes in the design bandwidth with all the others lying in between. We have plotted most of the other cases and will plot the remaining ones to confirm that the other cases do not produce any unexpected problems in roundoff sensitivity and gain.

B. CCD Topology

The CCD structure for the split electrode filters will be a four electrode per cell, double polysilicon device. To simplify the output sense circuitry we will use a clocking scheme which maintains two of the four electrodes per cell at dc potentials and that pulses the other two electrodes. The charge transfer process is illustrated in Figure 10. Here the surface potential is drawn (positive downward) to illustrate the potential wells for signal electron charge packets at various times in the clock cycle. At times t_1 the charges are shared under the ϕ_1 and ϕ_2 electrodes and the ϕ_1 and ϕ_2

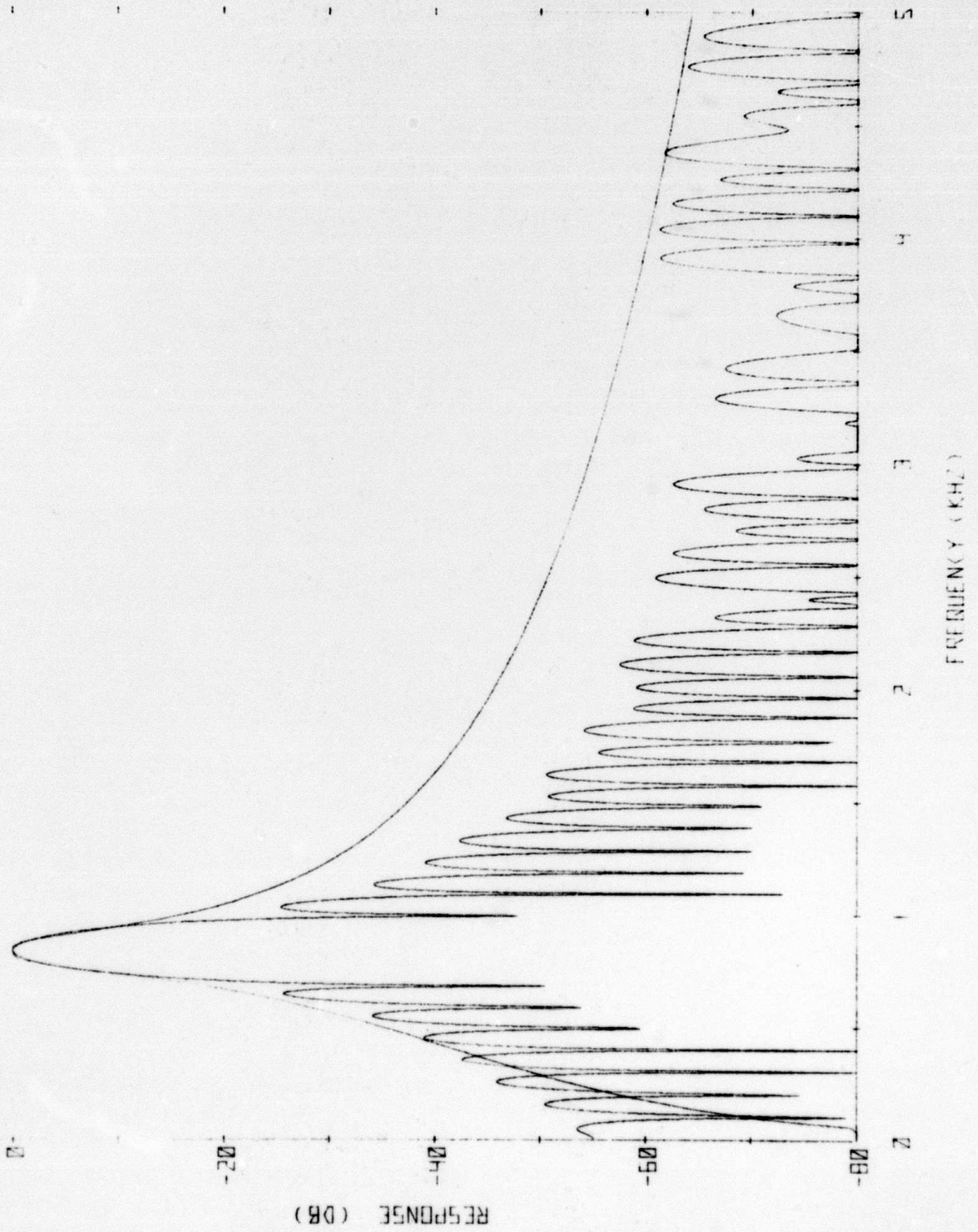


Figure 5 Analyzer Channel #6 Showing the Effects of Tapweight Roundoff

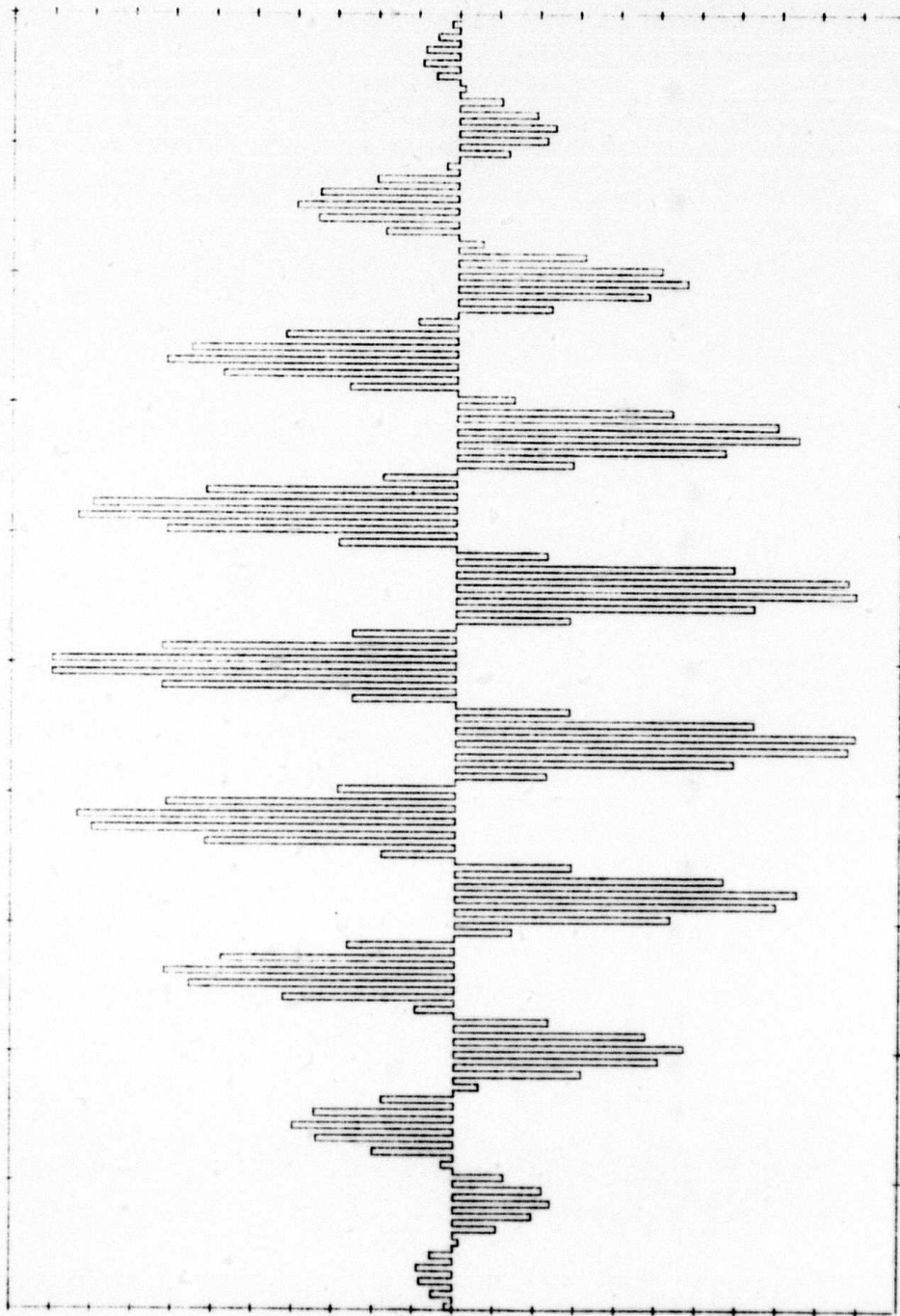


Figure 6 Weighting Coefficients for Analyzer Filter #6

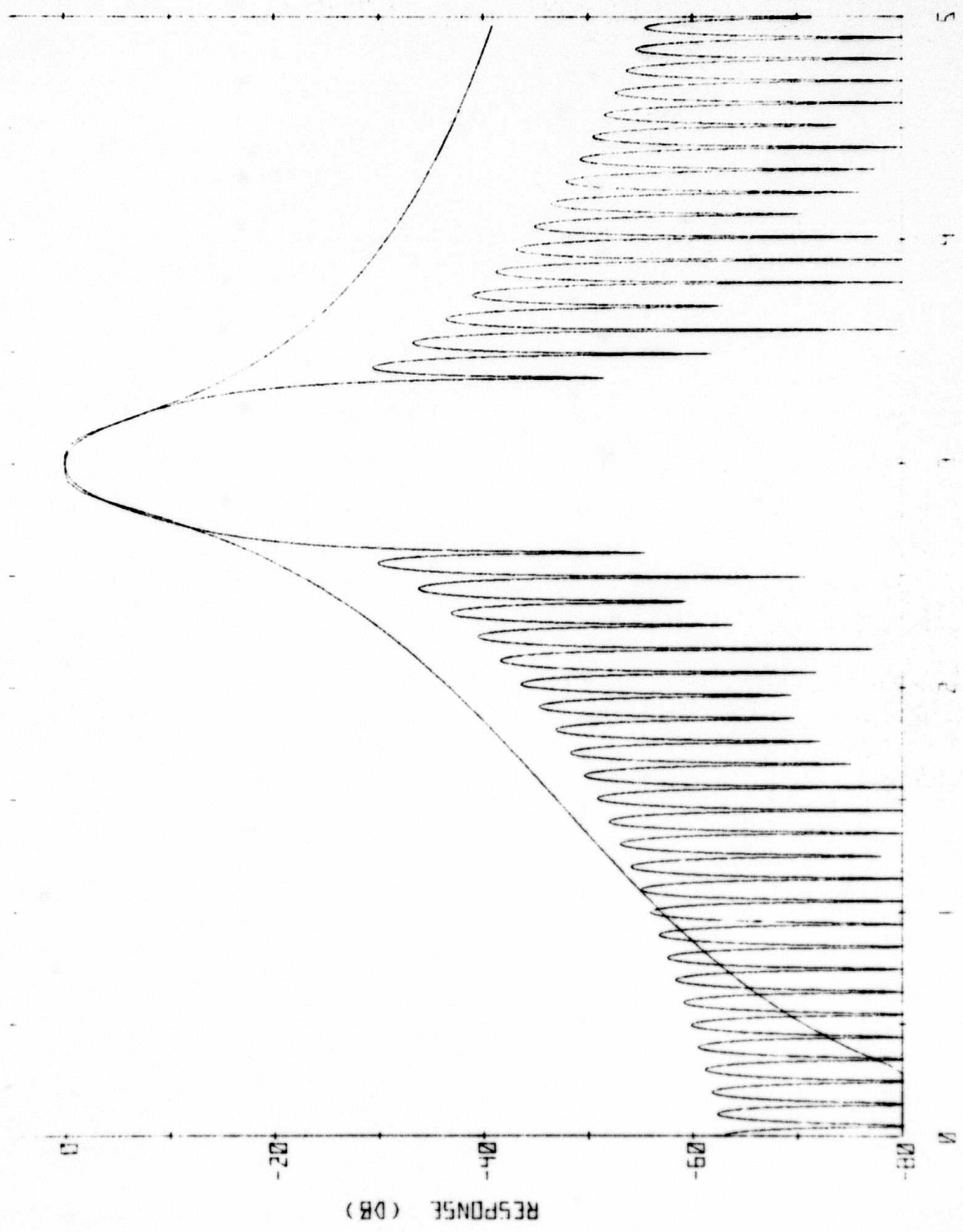


Figure 7 Analyzer Filter #17

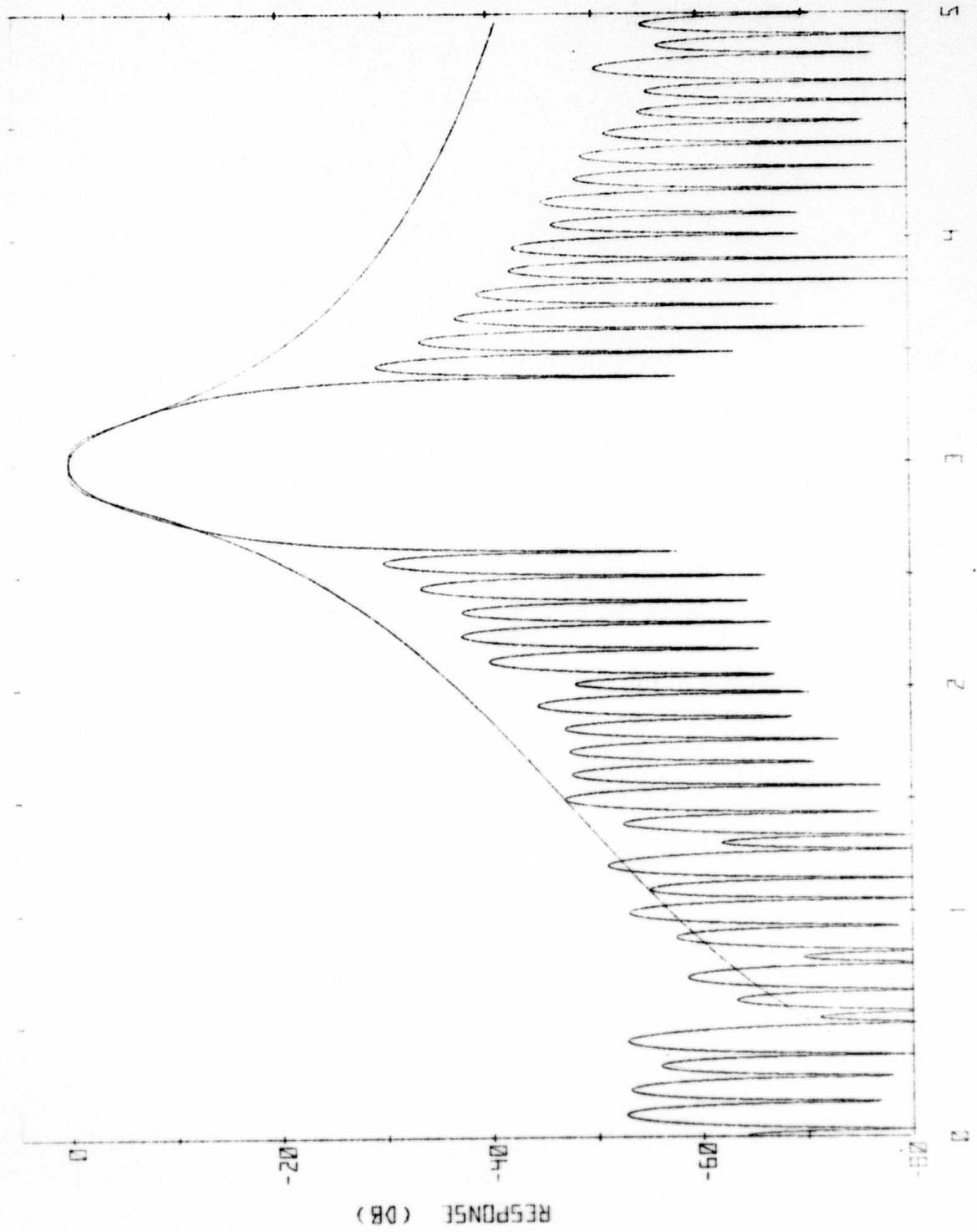


Figure 8 Analyzer Filter #17 with Tapweight Roundoff

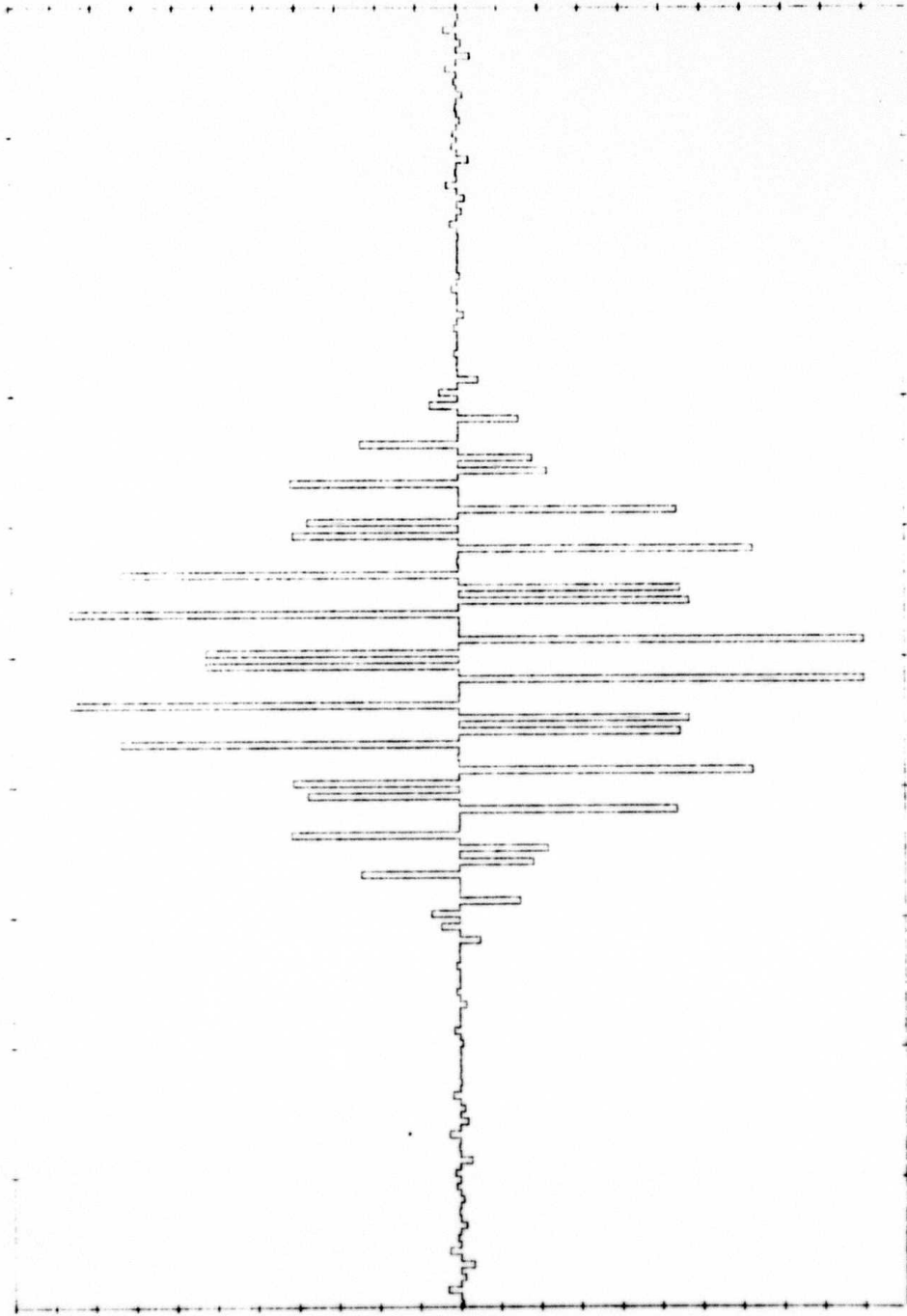


Figure 9 Tapweights of Filter #17

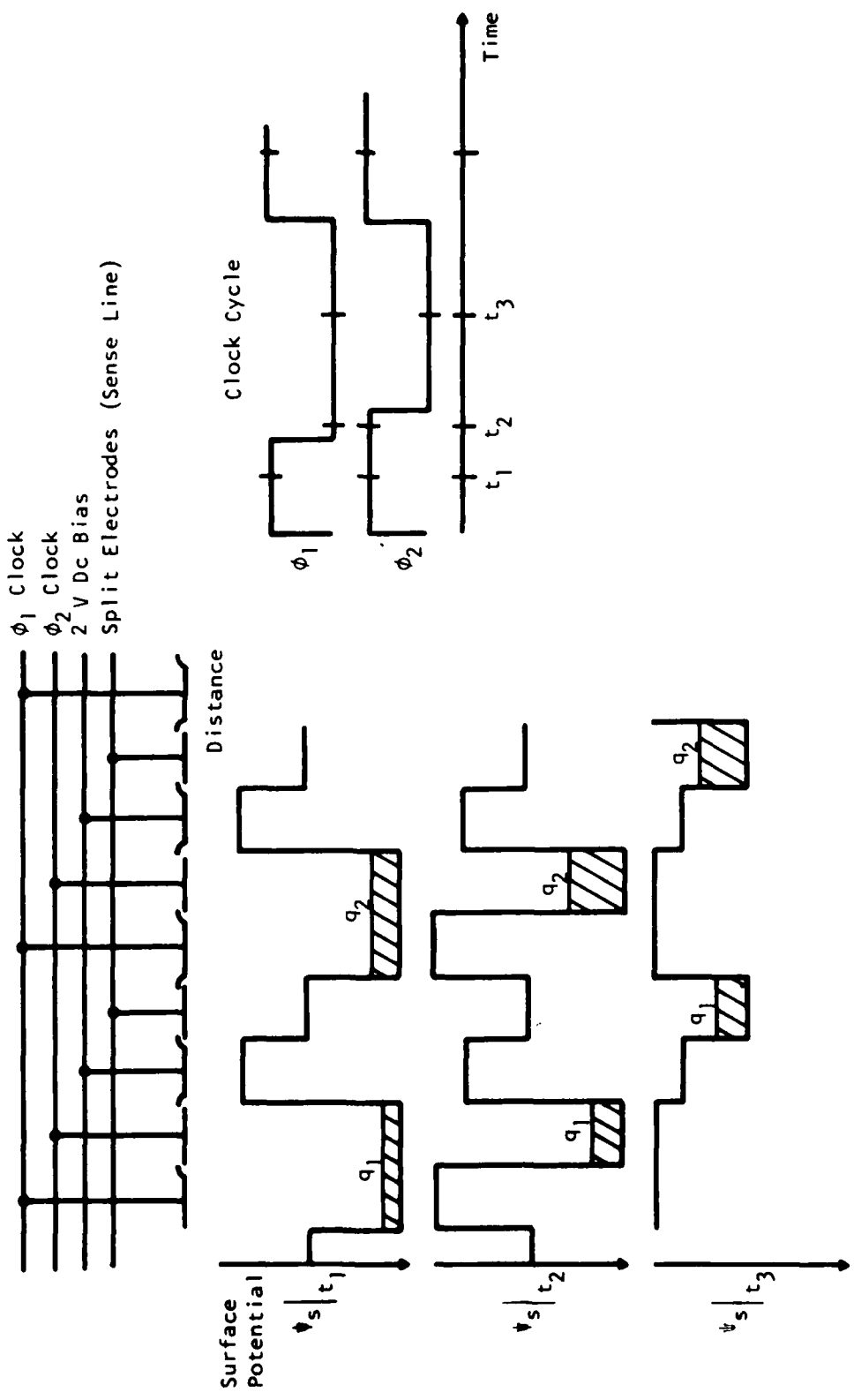


Figure 10 Schematic of CCD Charge Transfer Process and Clock Timing

clocks are ON (15 V). At time t_2 the ϕ_1 clock is in the OFF (0 V) state and the charge packets have moved forward to the wells under the ON ϕ_2 electrodes. At time t_3 the ϕ_2 clock is OFF and the charge packets have been pushed over the barrier created by the 2 V dc bias on the third electrode of each CCD cell and are stored under the sense electrodes. The sense electrodes are maintained at a constant dc potential (2.5 V) by the output circuit described below.

The output sense circuit is a charge integrating amplifier as illustrated in Figure 11. The difference in charge sensed by the two parts of each split electrode is proportional to the signal charge and to the difference in the area of the two pieces of the electrode. Thus the weighting coefficient is obtained by controlling the positions of the split in the electrode. The products of the weighted charge packets are summed by simply tying the electrodes to two summing bus lines which form the two inputs to the integrator. The output signal voltage is therefore

$$V_{out}(n) = \frac{1}{C_f} \sum_{k=1}^N h_k \frac{V_{in}(n-k)}{C_{in}},$$

in which C_{in} is the input capacitance of the CCD, h_k is the filter weighting coefficient, C_f is the gain determining feedback capacitor of the integrator, and n is the time index.

C. CCD Filter Amplifier

The CCD bandpass filters use the split electrode technique to implement the tapweights. This technique requires the use of an amplifier to sense the charge on the split clock lines differentially and provide a voltage output. This amplifier is called a differential current integrator (DCI). A schematic of the DCI used is shown in Figure 12. The amplifier functions as an integrator, integrating the CCD output signal onto the feedback capacitors, C_{FB} .

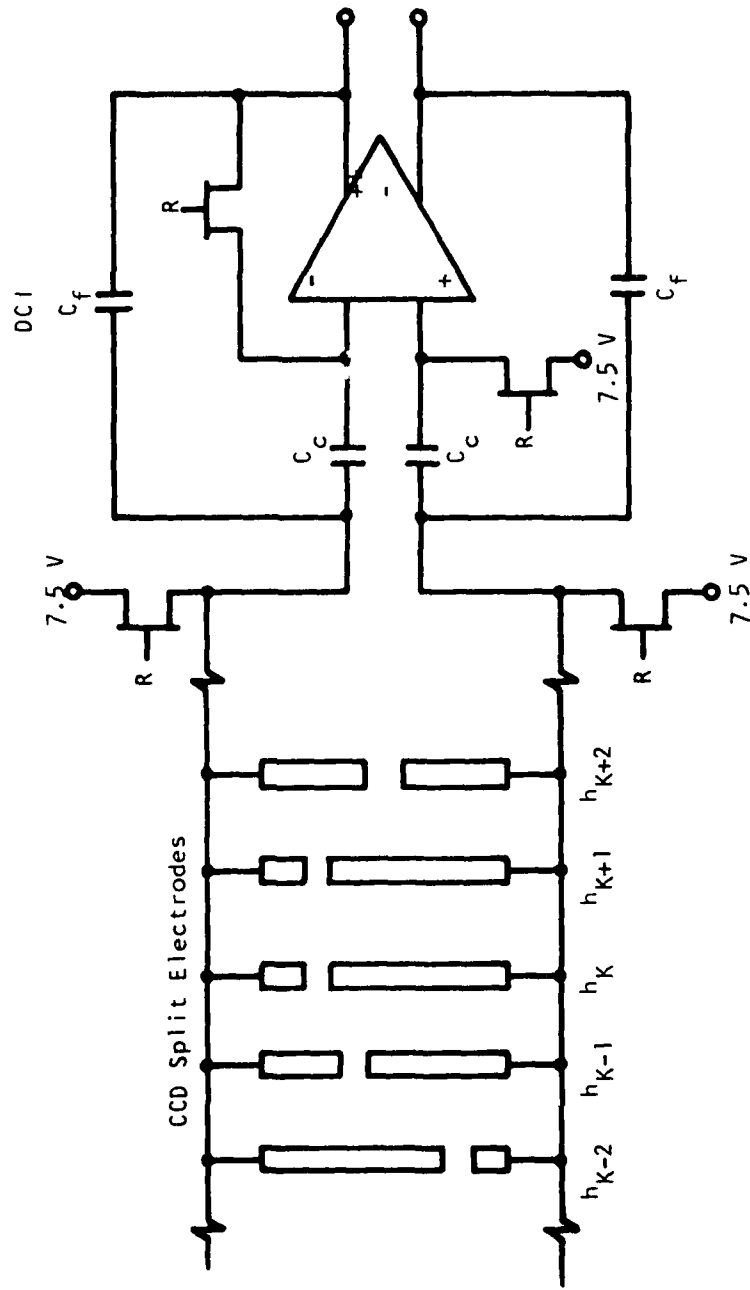


Figure 11 CCD Output Circuit. The differential current integrator (DCI) provides an output voltage.

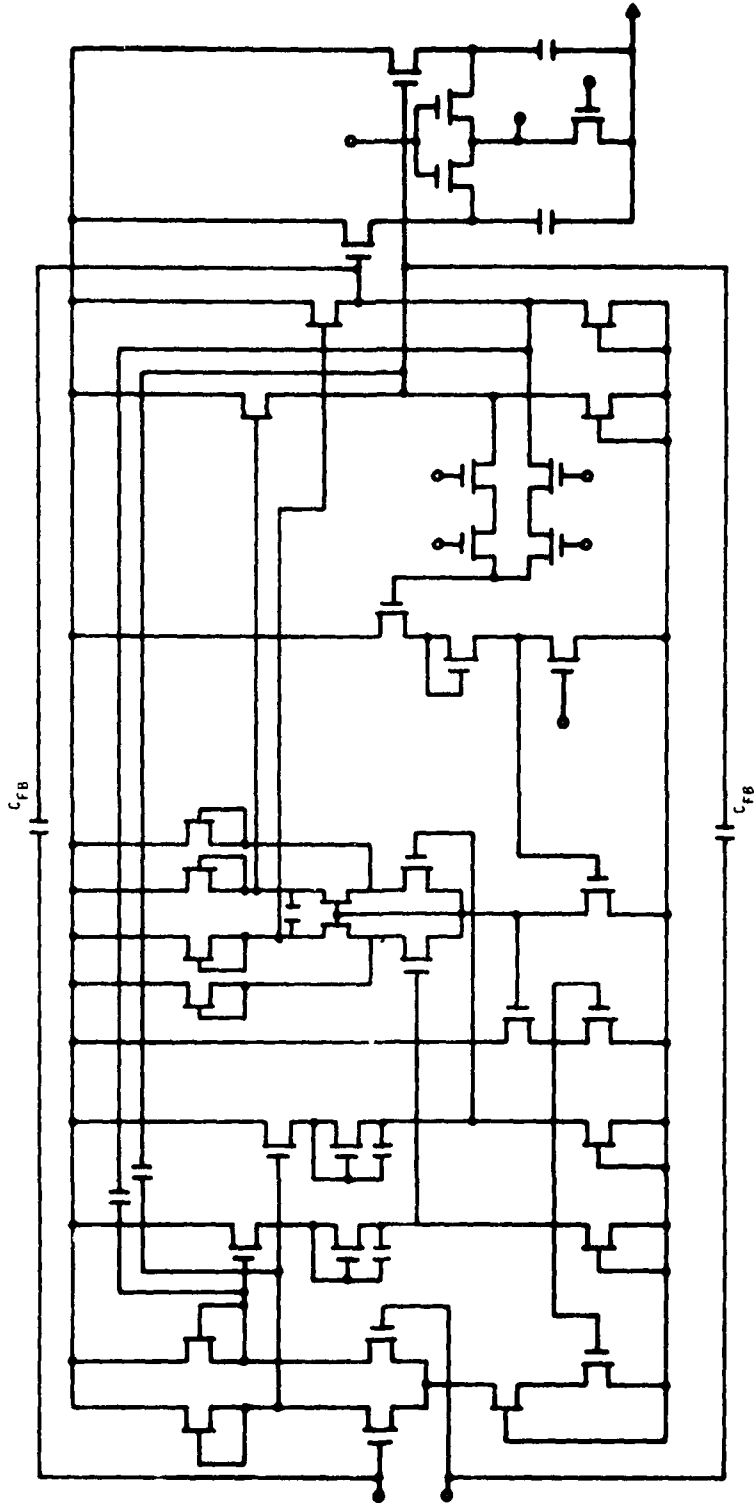


Figure 12 Amplifier/Rectifier

The amplifier has two stages of differential gain with source followers between the first and second stages. The outputs of the second differential stage are also buffered by source followers. The dc operating point and common mode rejection are obtained by two overlapping feedback loops connected to the current source of each differential pair.

From the outputs of the second stage to the outputs of the first stage are two compensating capacitors that make the second stage look like an integrator. These compensating capacitors create a dominant pole in the amplifier's frequency response. An additional compensating capacitor is placed between the second differential stage outputs to create a pole at high frequencies.

The DCI's open loop and loop transmission frequency responses are shown in Figure 13. From the loop transmission curve the phase margin and gain margin can be measured. The closed loop frequency response of the DCI for a gain of 100 is shown in Figure 14. The -3 dB frequency is 125 kHz.

Because the processing gain of each filter may be different due to different filter tapweights, the gains of the DCIs must be programmed. This can be accomplished by varying the size of the feedback capacitors. This will be done by calculating the gain required for each filter and computer generating the feedback capacitor.

A summary of the DCI amplifier characteristics is shown in Table 2.

D. Full-Wave Rectifier

The rectification technique is based on the capacitive source following. A source follower with capacitive load only will act as a half-wave rectifier if the capacitor at the source node of the transistor is precharged. When the voltage at the source reaches $(V_G - V_T)$, any signal with a level higher than

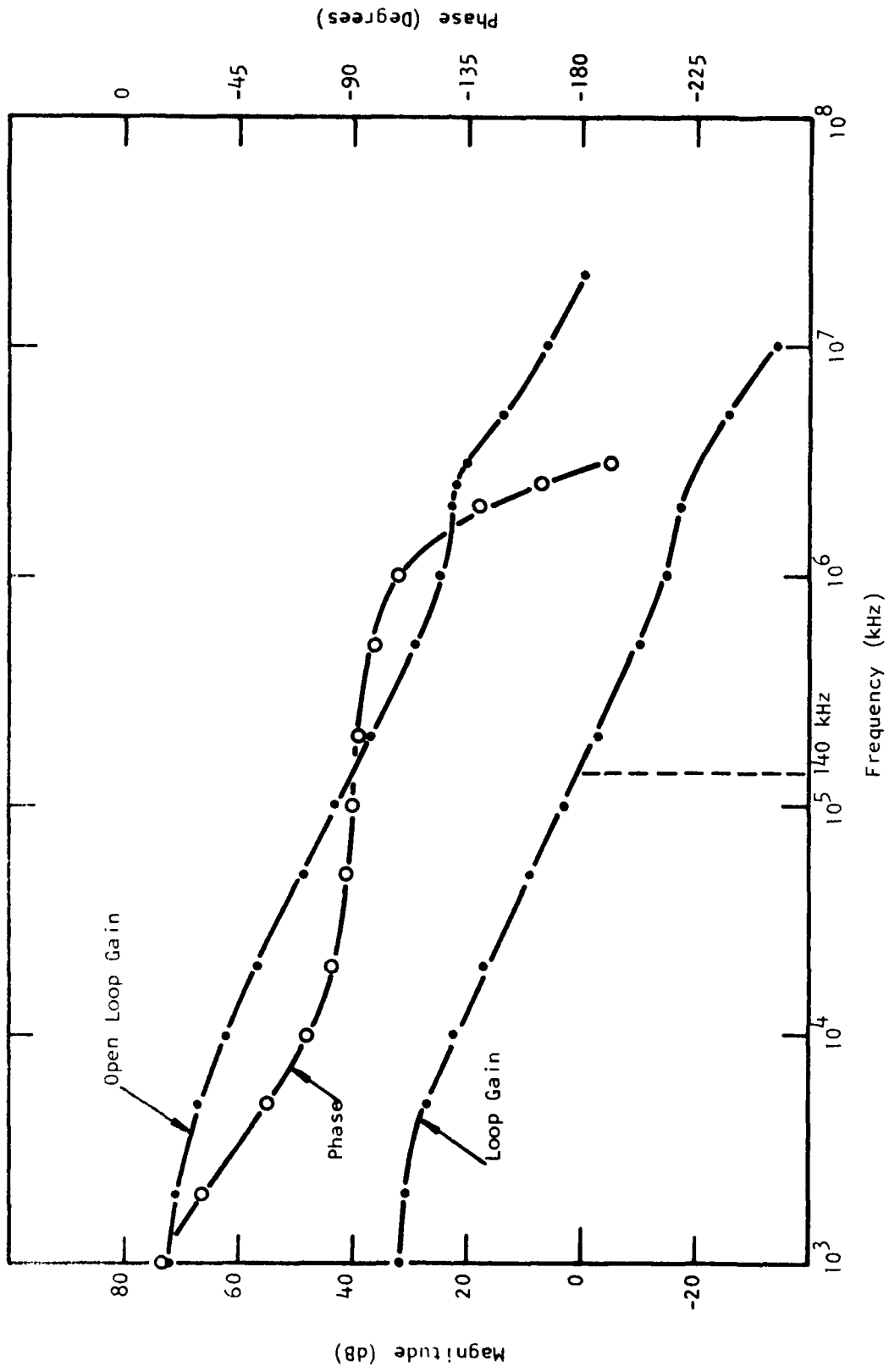


Figure 13 Amplifier Open Loop Frequency Response

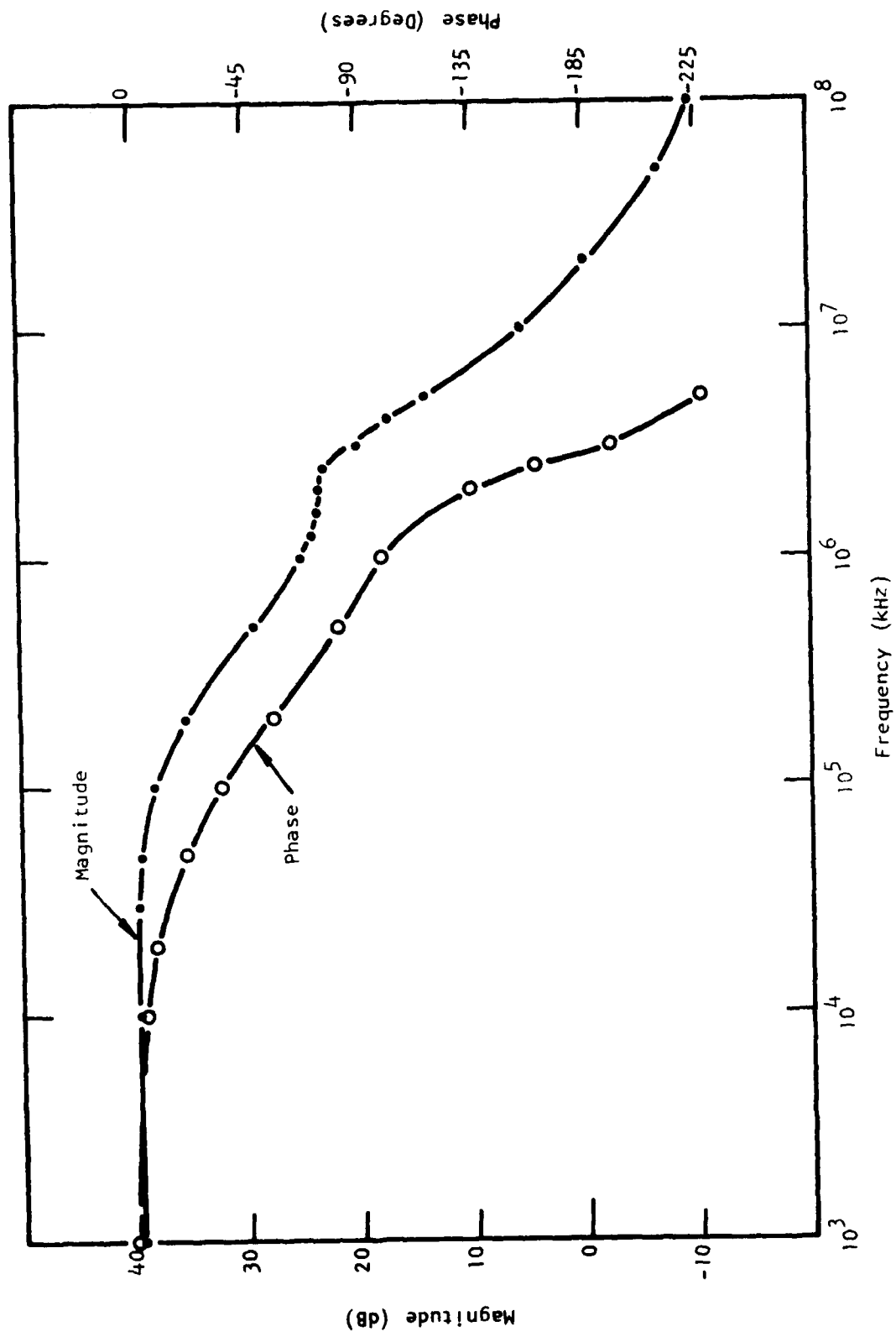


Figure 14 Amplifier Closed Loop Frequency Response

TABLE 2
DCI AMPLIFIER CHARACTERISTICS

Open loop gain	4100
Open loop bandwidth	4 kHz
Closed loop gain	50 → 100
Closed loop bandwidth	316 kHz → 125 kHz
Phase margin	90°
Gain margin	20 dB
Rise time (0 to 90% of 5 V output)	9 μs
Settling time (1%)	13 μs
Voltage swing	± 5 V
Power	6.5 mW
Area	0.23 x 1.27 mm ² (9 x 50 mil ²)

V_G will appear at the source while any signal with a level lower than V_G will cut off the transistor. Two capacitive source followers, together with signal inversion at one input, constitute a full-wave rectifier.

A circuit based on the above principle is shown in Figure 15. The operation of the circuit is as follow:

- (1) With the ϕ_R clock ON and ϕ_{R1} ON, the nodes A and A' are connected to $V_{ref 2}$ ($< V_G - V_T$) and node B is connected to $V_{ref 2}$.
- (2) With ϕ_{R1} OFF, node voltage at A and A' are charged up to $(V_G - V_T)$, respectively, while node B remains at $V_{ref 2}$.
- (3) With ϕ_R OFF and the complementary clock ϕ_R' ON, the signal appears at the output and the negative transient of ϕ_R is cancelled by the positive transients of ϕ_R' . Therefore the negative offset is eliminated.

The overall cycle thus consists of a reset phase, during which the offset voltage is stored on the capacitor and a zero signal appears at the output, followed by a signal phase, during which the rectified signal appears at the output.

To verify the rectification principle and the dc offset elimination technique, a circuit was built with discrete components. Figure 16 shows a rectified waveform. The breadboard version of the circuit showed that the dc offset could be reduced to such a level that a 4 mV rectified signal could be obtained and the signals from the two inputs had equal amplitude. Referred to the input, this corresponded to 20 mV input signal. Major limitation of the breadboard circuit was the stray capacitances. Therefore in the I-C version, where the effect of stray capacitances and feedthrough can be minimized, the circuit should have a wider dynamic range.

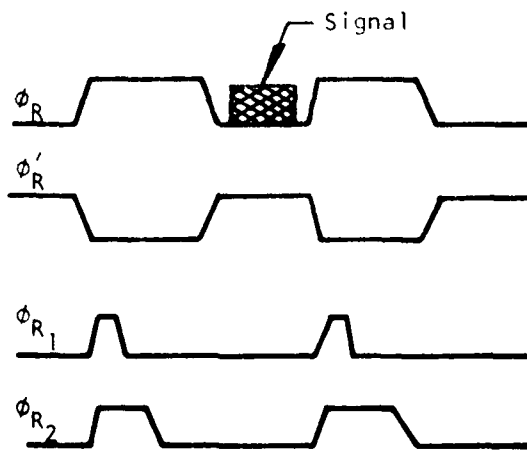
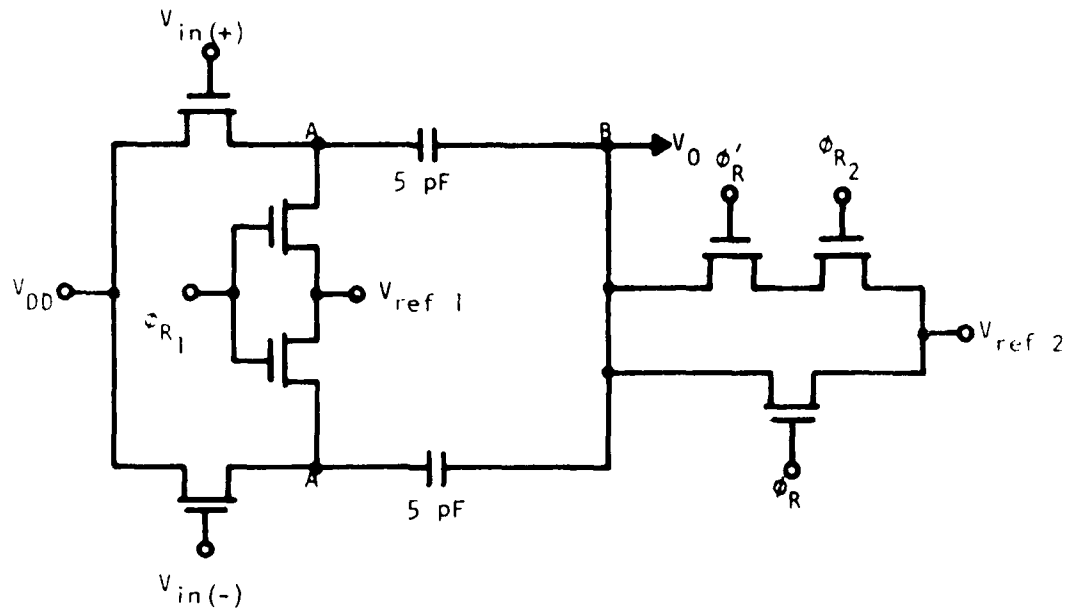


Figure 15 Full-Wave Rectifier Circuit and Timing Diagram

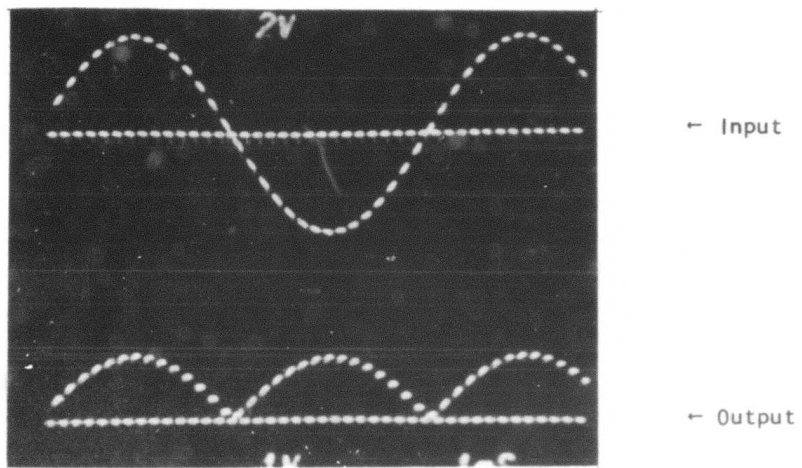


Figure 16 Rectifier Output Waveform
from Breadboard Simulation

E. Low-Pass Filter

The analysis chip requires a three-pole, Butterworth low-pass filter with $f_c = 35$ Hz to filter the output of the rectifier. A switched capacitor type, sampled-data, low-pass filter was designed to meet this requirement.

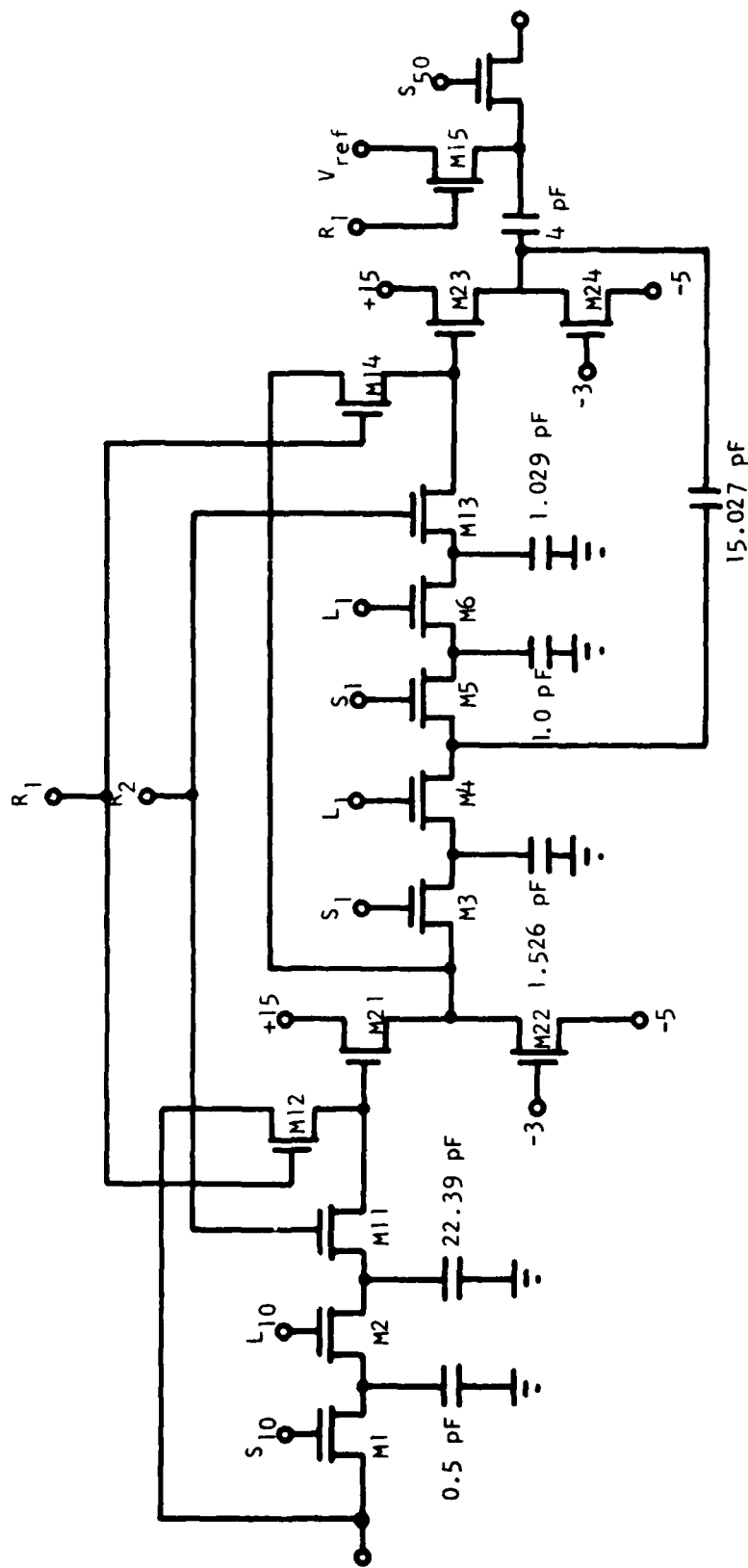
The circuit is shown in Figure 17. It consists of an R-C section in cascade with a Sallen-Key type, low-pass filter. The R-C section provides a real pole while the Sallen and Key section provides the remaining two complex poles. Different clock rates are used in the two sections in order to minimize the on-chip capacitor area. The R-C section is to be operated at a clock rate of 10 kHz while the clock rate for the Sallen and Key section is 1 kHz.

Because of the dc offset problem inherent with MOSFETs, it is necessary to use ac couple, dc restore techniques to eliminate the effect of V_T variation. With R_1 ON, R_2 OFF, the source followers are isolated from the rest of the circuit. The dc offset is stored on C_0 . With R_2 ON and R_1 OFF, every one-tenth of input data will appear at the output.

The circuit has been designed and simulated on IBM 370. Its total area is about 30×9 mil². The values of capacitors shown in Figure 17 represent a compromise between area and sensitivity.

F. Logarithmic A/D Converter

Signal dynamic range compression and analog-to-digital conversion are accomplished in the logarithmic A/D converter. The 19 low-pass filter outputs are multiplexed into the A/D converter at a 1 kHz rate. The converter output is a five-bit word with a $1\frac{1}{2}$ dB step size. Therefore the total dynamic range of input signal covered is 48 dB.



26

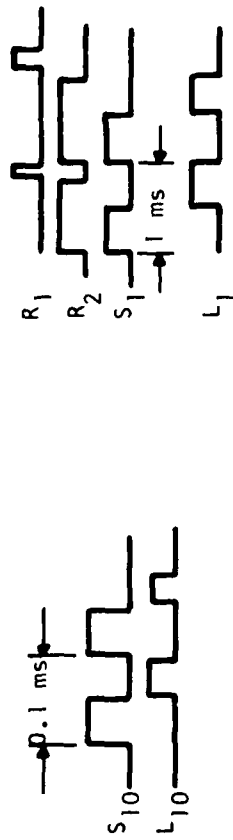


Figure 17 Low-Pass Filter

A block diagram of the converter is shown in Figure 18. Logarithmic response is obtained with an array of eight polysilicon capacitors ($C_0 - C_7$) weighted such that the sum

$$C_{\text{sum}} = \sum_{n=i}^7 C_n \text{ for } i = 0 - 7$$

is incremented in 6 dB steps and with a polysilicon resistive divider ($R_0 - R_3$) which makes available four reference voltages ($V_0 - V_3$) and a reset voltage V_{reset} spaced $1\frac{1}{2}$ dB apart to the capacitor array. A successive approximation technique is used to determine the digital word. A 10-stage shift register (SR10) clocked by 10 kHz pulses R10 and S10 continuously circulates a single "1" bit to provide sequencing for the A/D converter. When SR10₀ is high the converter goes through a reset cycle. At this time the latches containing the digital output ($Q_1 - Q_5$) are reset to "0" and the bottom plates of the capacitors $C_0 - C_7$ are clamped to V_{reset} while the signal amplifier and the high gain comparator A2 are reset. A signal from one of the 19 low-pass filter outputs is then applied to C_{sig} by the A1 amplifier. The signal is inverted by A1 and appears on node n_c attenuated by $\frac{1}{2}$ by the capacitor array. The comparator saturates in the high state if the signal is greater than ≈ 4 mV.

To determine the first three bits (Q_1, Q_2, Q_3) of the digital output, LATCH 1 through LATCH 3 are sequentially set to "1" by the shift register. When LATCH 1 is set, the CAPACITOR DECODE circuit causes the bottom plates of capacitors $C_3 - C_7$ to be switched from V_{reset} to V_{switch} ($V_{\text{switch}} = V_0$ at this time). This causes the voltage on node n_c to increase by an amount proportional to $C_3 + C_4 + C_5 + C_6 + C_7$ and to V_0 ($25\frac{1}{2}$ dB). If this voltage increase is greater than the decrease that was caused by the signal, then the comparator A2 will change state and at the end of this cycle the Q_1 output of LATCH 1 will be reset to "0." If the voltage increase is not enough to cause

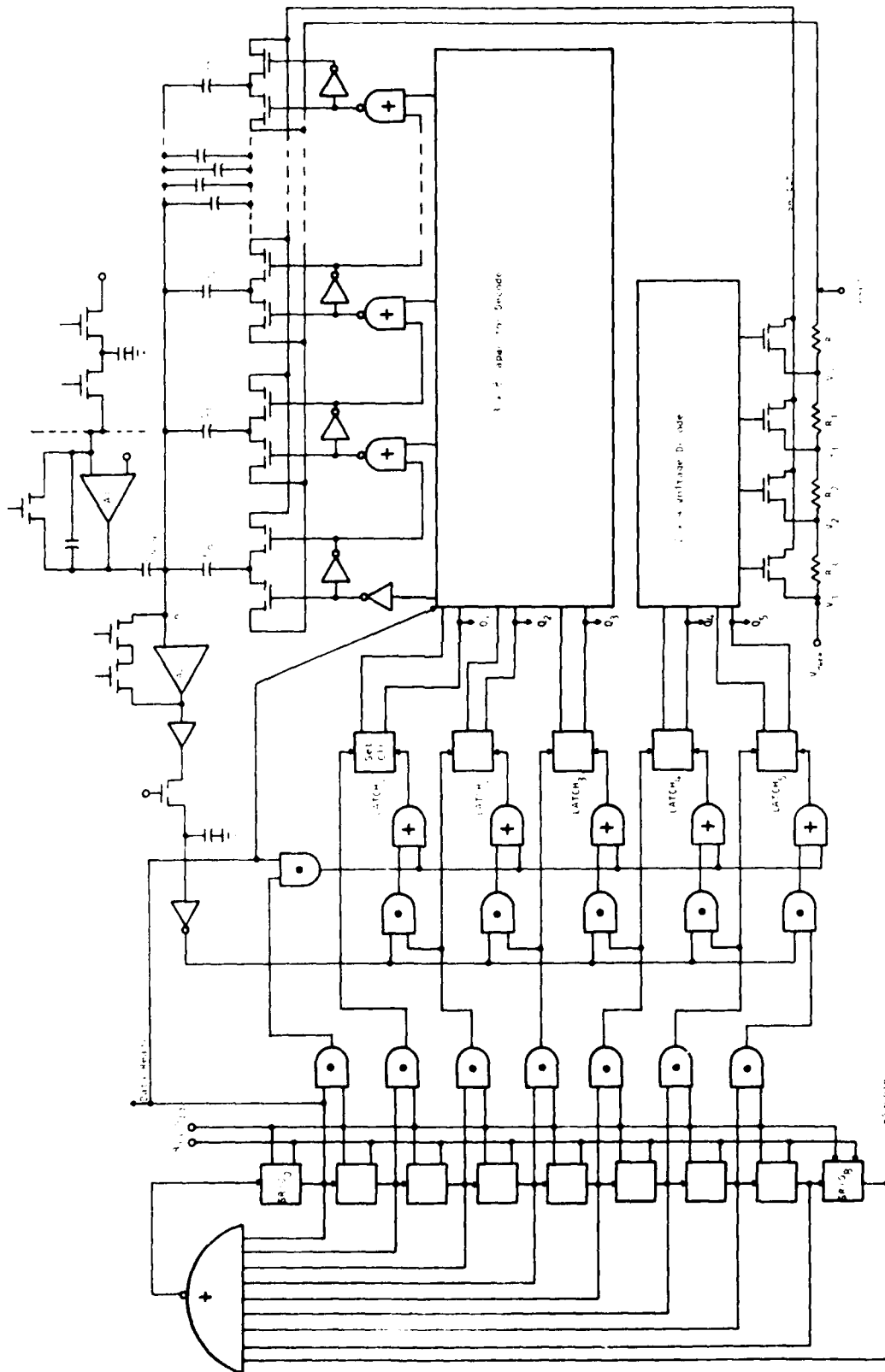


Figure 18 Five-Bit Logarithmic A/D Converter.

- 48 dB Dynamic Range
- $1\frac{1}{2}$ dB Step Size

the comparator to change state, then the Q_1 output of LATCH 1 will remain set to "1." Bits Q_2 and Q_3 are determined in the same fashion, after which the capacitors that bring the voltage on node n_c to within 6 dB below the comparator switching threshold remain clamped to V_{switch} . The other capacitors are clamped to V_{reset} . Next LATCH 4 is set causing the voltage V_{switch} to increase by 3 dB from V_0 to V_2 . This causes the voltage on node n_c to increase by 3 dB. If the comparator changes state, then the Q_4 output of LATCH 4 is reset to "0"; otherwise it remains "1." Q_5 is determined in the same way. The digital word is now completely determined and the shift register (SR10_g) causes the MOS to TTL converters to sample the word. SR10₀ provides a data-ready signal to the microprocessor which then has 800 μ s to read the word.

G. MOS/TTL Output Buffers

The analyzer A/D converter has six output signals, five data lines, and a data-ready signal. Each of these is buffered by an identical amplifier to provide TTL level outputs with a fanout of two standard loads. A computer model of the circuit indicates that each amplifier will dissipate 0.67 mW and that the rise and fall times under maximum load are 80 to 90 ns. Each amplifier consumes $0.65 \times 10^{-5} \text{ cm}^2$ (36 mil²) of surface area.

The schematic diagram of one of these drivers is shown in Figure 19. The circuit consists of two depletion load inverters, a flip-flop, and a push-pull output stage. Transistor pairs M1, M3 and M2, M4 form the two inverters. The inverted input signal appears on node A and the true signal reappears on node B where the levels now are 0 V and V_{DD} (15 V). These signals are applied to the load transistors (M5 and M6) of a flip-flop, and the outputs of the flip-flop drive the push-pull output stage (M9 and M10). Because the flip-flop and the push-pull stages are composed of enhancement mode devices, there is no quiescent current required, resulting in the low on-chip power dissipation.

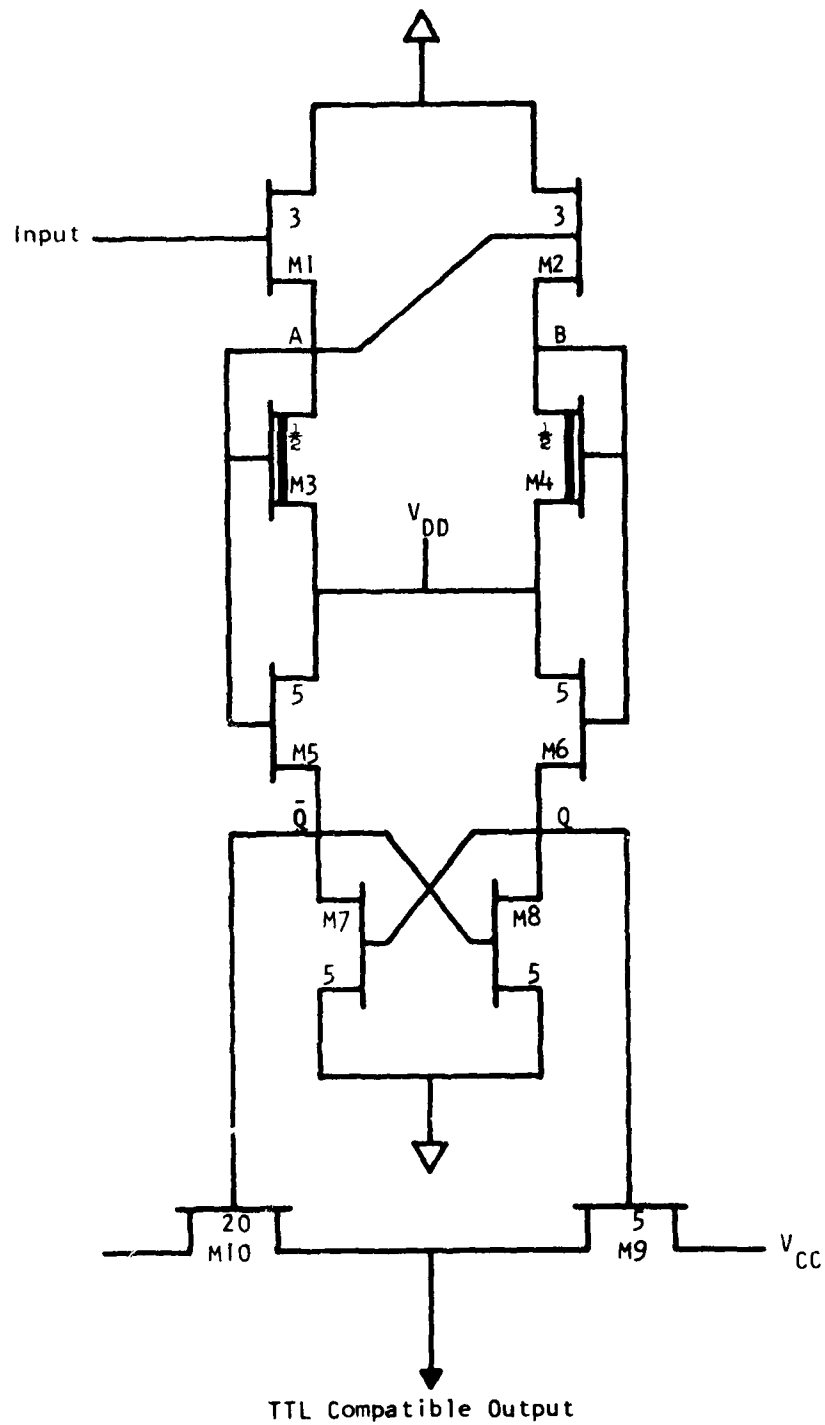


Figure 19 MOS to TTL Output Buffers

SECTION III
SYNTHESIZER IC

The synthesizer IC block diagram is shown in Figure 20. The details of this IC will be provided in a later report, but a brief general description will be provided below.

The synthesizer IC will have a D/A converter whose output will be demultiplexed into 19 sample-and-hold circuits, i.e., one for each channel of the synthesizer filter bank. Each sample-and-hold operates at the frame rate and the outputs of the sample-and-hold circuits are interpolated up to a 10 kHz sample rate by a two-stage low-pass filter similar to those in the analyzer IC. The outputs of the low-pass filters modulate the excitation of the corresponding channel bandpass filters. The bandpass filters will be a recursive switch capacitor, two-pole filter of the type shown in Figure 21. The excitation will be generated on chip from the digital input data. A PLA structure will provide the pitch period for voiced sounds and a pseudorandom sequence will provide the noise excitation. Summing of the channels will also be provided on chip as well as clocks for the filter functions.

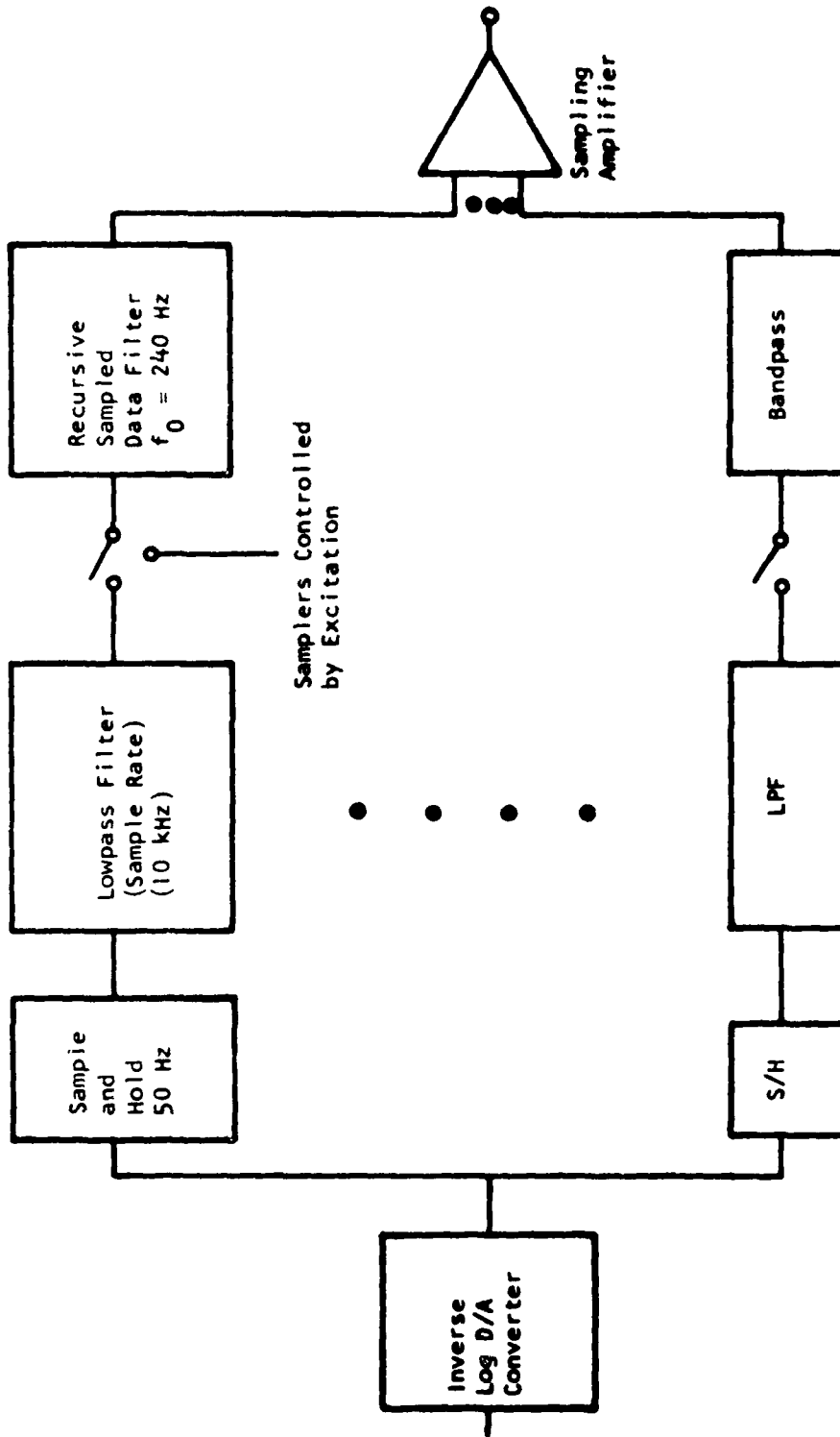


Figure 20 Synthesis IC

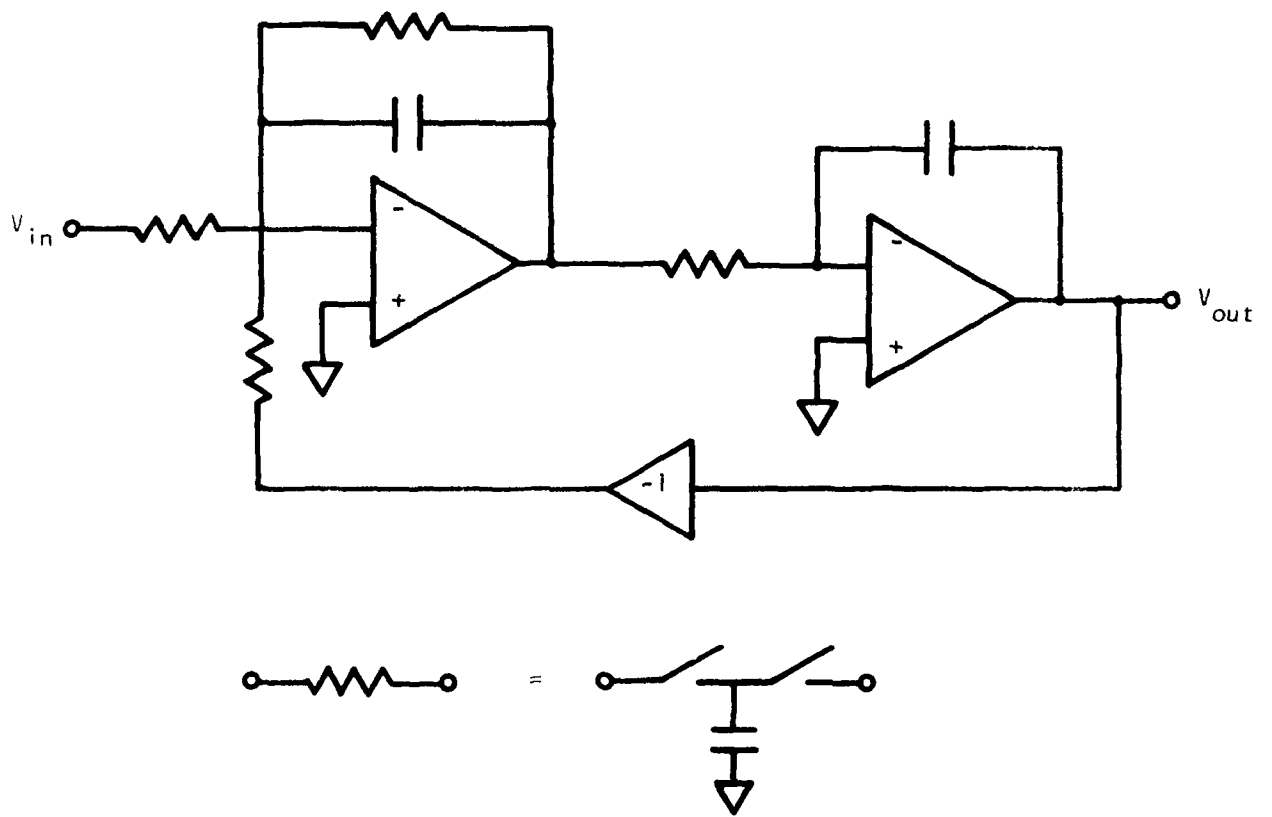


Figure 21 Two Pole Bandpass Filter

SECTION IV
STATUS AND PLANS

Our current development schedule is shown in Figure 22. As indicated, the analyzer chip circuit design is completed and the layout is in the final phase. There were recent delays that slipped our schedule about two weeks on the analyzer chip that were due to technical reasons.

- Analysis of the rectifier indicated there were potential offset problems that we have now solved.
- We made the decision to convert the design to a new simplified LCD fabrication process that we demonstrated in January and February. This process offers higher dynamic ranges, better amplifier performance, higher density, and higher yield and compatibility with production lines.

Currently we expect to complete chip fabrication of the analyzer ICs in early June and, after evaluation, ship some of them to Lincoln Laboratory for testing by the end of July. We will continue extensive testing and evaluation throughout the remainder of the program to aid in redesign activities later.

The synthesizer IC will use many of the same circuit elements as the analyzer IC, e.g., op amps, capacitive array for the D/A converter. The filter bank is being designed now and we expect to start bar layout by the first of May. The fabricated ICs should be completed by mid-September and we expect to be able to deliver the synthesizer ICs to Lincoln Labs for evaluation.

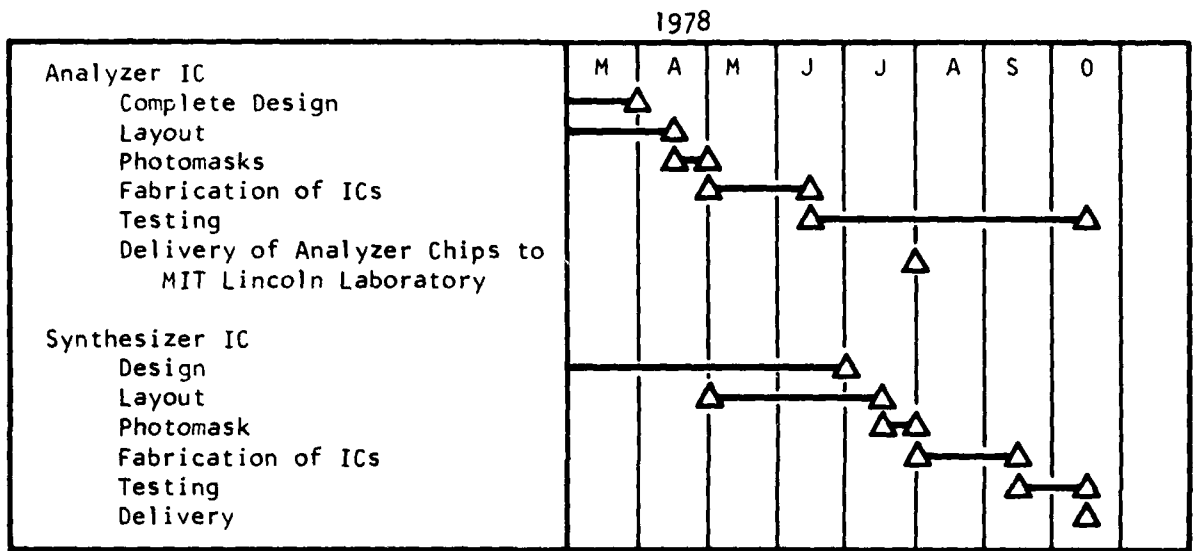


Figure 22 Belgard Chip Development Schedule